Hydrogen production using vinasse as sacrificial agent and Pt/TiO2 as photocatalyst under UV irradiation

Patricia Ferreira Silvaino
Instituto de Pesquisas Energeticas e Nucleares
João Coutinho Ferreira
Instituto de Pesquisas Energeticas e Nucleares
Saulo Amaral Carminati
saulocarminati89@gmail.com
Instituto de Pesquisas Energeticas e Nucleares https://orcid.org/0000-0001-8429-8788
Jorge Moreira Vaz
Instituto de Pesquisas Energeticas e Nucleares
Estevam Vitorio Spinacé
Instituto de Pesquisas Energeticas e Nucleares https://orcid.org/0000-0002-7011-8261

Short Report

Keywords: vinasse, photochemistry, photocatalysis, UV irradiation, Pt/TiO2

Posted Date: October 28th, 2024

DOI: https://doi.org/10.21203/rs.3.rs-5240232/v1

Abstract

Vinasse, a dark-colored aqueous byproduct of bioethanol production, contains a variety of organic compounds and inorganic salt ions. In this study, vinasse was utilized as a sacrificial agent in the water splitting reaction using Pt/TiO□ as a photocatalyst under UV irradiation. The gaseous products generated were analyzed, revealing the formation of hydrogen (H□) along with other gases, including CO□, CH□, CO, C□H□, C□H□, C□H□, and C□H□□. When using filtered vinasse as the sacrificial agent, H□ and other gaseous products were produced solely through photolysis, even in the presence of the Pt/TiO□ photocatalyst. Notably, H□ production from the water splitting reaction was enhanced when inorganic salt ions were removed from the vinasse, and a lower concentration of vinasse was employed in the reaction medium.

Introduction

The main source of raw materials for the chemical industry is still fossil fuels; however, environmental impacts have stimulated the use of renewable sources. In this sense, agricultural biomass and wastes have attracted a lot of interest. Brazil is the second largest producer of bioethanol that was mainly obtained by sugarcane fermentation generating vinasse as the main residue. Vinasse is an aqueous dark-colored waste containing organic compounds (residual sugars, glycerol, mannitol, organic acids and phenolic compounds) and inorganic salt ions (sodium, potassium, calcium and magnesium cations and chloride, nitrate, nitrite, phosphate, and sulfate anions). Due to the large volumes of vinasse resulting from bioethanol production, at least 10–15 liters for 1 liter of ethanol, its disposal and/or use become a major challenge. In Brazil, during the 1980s, fertigation became a widespread practice, leading to soil salinization and the leaching of metals into groundwater [1, 2].

More recently, other processes like anaerobic digestion of vinasse to produce biogas are being evaluated and developed [3, 4]. Also, the vinasse photocatalytic degradation for decolorization and total organic carbon removal is another process that has been extensively investigated [5, 6].

The photocatalytic water splitting over nanostructured semiconductors for H_2 production has the advantage of renewable energy utilization and a common strategy is the use of sacrificial agents (SAs) like methanol, ethanol and others to overcome the large thermodynamic barrier of oxygen evolution reaction and the recombination of photogenerated charge carriers [7]. On the other hand, the high cost of SAs is an obstacle to achieve practical applications and the low cost and easily accessible SAs like biomass and organic wastes become extremely interesting [8].

Despite the use of biomass-derived substrates like, glucose, polysaccharides, lignin and cellulose as SAs for photocatalytic H_2 production [7, 9–13], the use of raw wastes has been little explored [14]. The use of vinasse as a sacrificial agent in the water splitting process for hydrogen production over semiconductor-based photocatalysts has not yet been explored [5].

In this work, we explore the use of vinasse as sacrificial agent and Pt/TiO_2 as photocatalyst for H_2 production using UV irradiation. This approach could not only mitigate waste by improving resource

efficiency but also contribute to more sustainable energy systems.

Novelty Statement

To the best of our knowledge, this is first time that vinasse was used as sacrificial agent in the water splitting process.

Materials and Methods

Materials

The following reagents and solvents were used: TiO_2 P25 (Evonik), $H_2PtCl_6.6H_2O$ (Sigma-Aldrich®), Ethylene glycol (Dinâmica Química), ultrapure deionized water (18.2 MΩ cm, 25°C) and Ethyl alcohol (Sigma-Aldrich®, 99.5% purity).

Vinasse treatment

Raw Vinasse from Usina Colombo, Ariranha, São Paulo State, Brazil, was filtered (Vinasse F) on a paper filter to separate the liquid phase from the solid phase. In a further step, the inorganic metal salts (cations and anions) of the vinasse F were removed by ion-exchange (IE) process passing through a column of cation exchange resin (Amberlite IRC-748) and a column of anion exchange resin (Dowex-3) to remove the ionic species.

Synthesis and Characterization of Pt/TiO photocatalyst

The Pt/TiO_2 photocatalyst was prepared with 0.5 wt% of Pt content by an alcohol-reduction method [15, 16]. $H_2PtCl_6.6H_2O$ was dissolved in an ethylene glycol:water solution (3:1 v/v) and the TiO_2 P25 was dispersed in this solution. The resulting mixture was stirred and heated under reflux for 2 h. Afterwards, the mixture was centrifuged, and a light gray solid was obtained. The solid was washed with excess deionized water and dried at 90°C for 24 h.

The elemental composition of the Pt/TiO_2 was determined by WD-XRF (Wavelength-Dispersive X-ray Fluorescence) in a Rigaku Supermini200 spectrometer (Pd source, 50 kV, 200 W, Zirconium filter) using a calibration curve. The shape, size and dispersion of the Pt nanoparticles on the TiO_2 support were analyzed by TEM (Transmission Electron Microscopy) using a JEOL microscope, model JEM-2100 (200 kV). Photoluminescence (PL) spectra were performed in an Ocean Optics 2000 luminescence spectrometer + USB spectrometer with a CCD camera, from 200 to 1000 nm. The excitation wavelength was 265 nm, and the spectra were recorded at room temperature in the range of 200–1000 nm, with the scanning speed at 1000 nm min^{-1}, and the PMT voltage was 650 V. Raman spectroscopy measurements were obtained with a Horiba Scientific MacroRam Raman spectrometer using a 785 nm wavelength laser.

UV-Vis spectra of the vinasse solution before and after UV irradiation were recorded by using a Varian UV-Vis spectrometer model Cary 50 from 200 to 800 nm.

Photoconversion experiments

The photoconversion experiments were performed in system using a commercial Ace 250 mL photoreactor coupled with a gas chromatograph (GC) Agilent 7890B-mass spectrometer MSD 5977B system. The GC has a thermal conductivity detector (TCD), a methanizer and a flame ionization detector (FID). Two columns were used in order to separate the reaction products, a plot U and molecular sieve 5 Å column. Calibration curves were made using two certified gas mixtures to quantify CO_2, C_2H_4, C_2H_6, C_3H_8, C_4H_{10}, H_2, CH_4 and CO. The detection limits were 0.001% for CO_2 and C_2-C_4; 0.008% for CH_4 and CO and 0.3% for H_2. In a typical experiment, 75 mg of the Pt/TiO_2 photocatalyst was dispersed in 250 mL of an ethanol/water or vinasse/water solution (v/v) and a continuous flow of He gas (25 mL.min^{-1}) was bubbled into this suspension for 16 h before the beginning of the experiment to purge the O_2. During the entire photoconversion tests, He (25 mL.min^{-1}) was used as carrier gas and a 450 W Hg lamp (UV A/B/C) as a light source. Two cooling systems were used, one for cooling the Hg lamp operating at 40^{o}C and one coupled to a condenser at the output of the reactor connected to the CG system to condense the water (15^{o}C). In this manner, the photoconversion reactions were performed at a temperature close to 50^{o}C.

Results and Discussion

For Pt/TiO_2 photocatalyst, the Pt amount determined by WDXRF was 0.52 wt%, very close to the nominal value. Figure 1 shows the TEM micrograph and histogram of Pt/TiO_2 photocatalyst, where it can be seen the Pt nanoparticles (small black dots) with a good dispersion loaded on TiO_2 support and with sizes in the range of 2–5 nm.

The PL spectra of Pt/TiO_2 photocatalyst and TiO_2 P25 support are shown in Fig. 2 and present similar profiles with emission peaks centered at 431 and 436 nm for Pt/TiO_2 and TiO_2 P25, respectively. The emission peak of Pt/TiO_2 photocatalyst presented a lower intensity than the peak of the TiO_2 P25 support, indicating a decrease in the recombination rate of the electron-hole pair [17, 18].

The Raman spectra for Pt/TiO_2 photocatalyst and TiO_2 P25 support are shown in Fig. 3. The spectrum of TiO_2 P25 presented peaks centered at 140, 196, 394, 514 and 636 cm^{-1}, which are assigned to the vibrational modes of the anatase phase and the presence of a small peak at 445 cm^{-1} due to the presence of a rutile phase. These peaks are characteristic of TiO_2 P25 support that contains a mixture of both anatase and rutile phases [19, 20]. Pt/TiO_2 photocatalyst presented a similar profile but with a small positive shift of 3 cm^{-1} in the most intense peak, which was associated with the interactions between Pt nanoparticles the TiO_2 support, according to the literature [21, 22].

The photoconversions experiments are shown in Table 1. For comparative purposes, it was also studied the use of ethanol as a sacrificial agent (SA) in similar conditions.

Table 1
Products formation rates in the gas phase of vinasse and ethanol photoconversion (75 mg of photocatalyst, 250 mL SA + H_2O, 25 mL min^{-1} He, 450 W Hg lamp)

Sacrificial agent (SA)/ Photocatalyst	SA/H_2O (v/v)	Products formation rates (μmol. g^{-1} h^{-1})							
		C_2H_6	C_2H_4	C_3H_8	C_4H_{10}	CH_4	CO	CO_2	H_2
Vinasse F/without	50/50	407	12	123	21	157	909	4148	2004
Vinasse F/(Pt/TiO_2)	50/50	512	23	163	24	178	994	5248	2200
Vinasse IE/without	50/50	2113	159	552	257	1792	973	13254	2827
Vinasse IE/(Pt/TiO_2)	50/50	2089	224	591	280	1665	1096	15759	4619
Vinasse IE/without	10/90	572	9	166	56	1068	527	4449	1787
Vinasse IE/(Pt/TiO_2)	10/90	422	20	147	46	963	530	5685	5252
*Ethanol/without	50/50	863	6	94	13	1840	4545	236	32111
*Ethanol/(Pt/TiO_2)	50/50	4004	45	340	46	7148	13070	2176	145662

* *for comparative purposes*

Initially, vinasse F (the liquid phase was separated from the solid phase by filtration) was tested as SA using a SA:H_2O ratio of 50/50 (v/v) under UV irradiation. The products identified in the gas phase presented the following order of formation rates: $CO_2 > H_2 > CO > C_2H_6 > CH_4 > C_3H_8 > C_4H_{10} > C_2H_4$ and these products were formed by photochemical reactions (photolysis); since no Pt/TiO_2 photocatalyst was added in the reaction medium. On the other hand, the addition of Pt/TiO_2, the most common reference photocatalyst using UV irradiation [23], practically did not change the products formed or their formation rates and even doubling the amount of Pt/TiO_2 photocatalyst (150 mg) the results did not change. UV-Vis absorption spectra of vinasse (F) solution (50/50), after UV irradiation and after UV irradiation in the presence of Pt/TiO_2 as photocatalyst are shown in Fig. 4.

The UV-Vis spectrum of vinasse (F) showed absorption bands in the UV region (200–400 nm) and their intensities were reduced after the photoreaction under UV irradiation showing the degradation of vinasse by photolysis. However, when the photoreaction was performed in the presence of Pt/TiO_2 as photocatalyst, the intensities and the shape of the absorption bands were very similar to those of the

reaction carried out only in the presence of UV light showing the predominance of the photochemical reactions (photolysis) even in the presence of the photocatalyst. Therefore, in these conditions, the H_2 production comes mainly from the photolysis of vinasse rather than from water splitting reaction.

Vinasse contains appreciable amounts of inorganic salt ions[2] and some of these ionic species could absorb UV light in aqueous solution [24], as well as, can lead to deactivation of the photocatalysts [25, 26]. In order to eliminate the influence of these species, vinasse F was treated by an ion-exchange process (IE) and tested as SA (SA:H_2O ratio of 50/50) under UV irradiation and, in this way, an increase of all products formation rates was occurred in comparison with vinasse F. Interestingly, when this photoreaction takes place in the presence of Pt/TiO_2 photocatalyst and under UV irradiation, an increase in the CO_2 and H_2 (4619 μmol. g^{-1} h^{-1}) formation rates was observed, while the formation of other products practically remained unchanged. Thus, two simultaneous processes may be occurring, a photochemical and a photocatalytic process, which leads to an increase in CO_2 and H_2 production.

Recently, Wongyoong et al. [14] described the green synthesis of H_2 and the decolorization of distillery effluent using Au/TiO_2 as photocatalyst; however, neither H_2 production nor decolorization were achieved using the fresh distillery effluent even in the presence of the photocatalyst and UV irradiation. In the studied conditions, the maximum H_2 production (52.5 μmol. g^{-1} h^{-1}) with 64.4% decolorization was achieved only with 100-fold diluted distillery effluent and adding 15 vol% of ethanol, which is also a sacrificial agent, in the reaction medium. In a similar study, Iervolino et al. [27] described the simultaneous valorization and treatment of olive mill wastewater (OMW) by means of a photocatalytic process to produce hydrogen and decrease the polluting load of this waste using a home-made sol-gel TiO_2 as photocatalyst. The best results were obtained using a dilution of the OMW of 1:70 with deionized water assuring a H_2 production of about 4200 μmol. L^{-1} h^{-1}.

In this way, the volume of vinasse IE (SA:H_2O of 10:90) was reduced in the reaction medium (Table 1). Under UV irradiation a decrease in all products formation rates was observed compared to SA:H_2O ratio of 50:50. On the other hand, when the photoreaction was performed in the presence of Pt/TiO_2 photocatalyst, a more pronounced increase in the CO_2 and H_2 formation was observed. UV-Vis spectra of vinasse (IE) (10/90) after UV irradiation and after UV irradiation in the presence of Pt/TiO_2 as photocatalyst are shown in Fig. 5.

The intensities of the absorption bands of the photoreaction performed in the presence of Pt/TiO_2 photocatalyst were reduced compared to the one performed only under UV irradiation, indicating more effective vinasse degradation. Under these conditions, the use of a lower concentration of vinasse appears to facilitate the UV light absorption by the photocatalyst and makes the H_2 production through the water splitting reaction more effective.

For comparative purposes we also tested ethanol as SA (ethanol/water of 50/50) in the reaction medium. Under UV irradiation and in the absence of Pt/TiO_2 photocatalyst, an appreciable H_2 formation rate of 32

mmol g^{-1} h^{-1} was formed by photochemical reactions (photolysis). On the other hand, a remarkable increase of all products formation rates occurred in the presence of Pt/TiO_2 photocatalyst with a H_2 production rate of 145 mmol g^{-1} h^{-1}. Thus, even using an ethanol/H_2O ratio of 50/50, about 2/3 of the products formed came from the photocatalytic process, while for vinasse as SA, in these conditions, the photochemical processes are dominant. Probably, some organic or inorganic compounds of vinasse could inhibit the UV light absorption by the photocatalyst and/or block the surface catalytic sites [28].

Conclusions

The liquid phase of raw vinasse (vinasse F) was utilized as a sacrificial agent (SA) in the water-splitting reaction (SA/H_2O ratio of 50/50) under UV irradiation, resulting in the production of H□, CO□, CO, and C□-C□ hydrocarbons through a photochemical process. The presence of the Pt/TiO□ photocatalyst did not alter the products or their formation rates, suggesting that no photocatalytic activity occurred in these conditions. In contrast, using ion-exchanged vinasse (vinasse IE) as the SA under UV irradiation in conjunction with the Pt/TiO□ photocatalyst, led to an increase in H□ and CO□ production, indicating that photocatalytic processes were indeed occurring; however, the photochemical process still remained dominant. In the studied conditions, photocatalytic H□ production was enhanced using vinasse IE and reducing its concentration in the reaction medium (SA/H_2O ratio of 10/90). Therefore, further investigation into the use of vinasse as an SA is warranted, and ongoing studies aim to optimize process conditions and identify more effective photocatalysts.

Declarations

Funding and Acknowledgments

The authors gratefully acknowledge support from São Paulo Research Foundation (FAPESP - Grant number 2021/01896-4) and from Brazilian National Council for Scientific Development (CNPq - Grant number 407967/2022-2 and 384264/2023-9). We also thank the support given by Arthur P. Machado from “Laboratório de Nanotecnologia e Energia Solar”, Chemistry Institute, UNICAMP for providing the facilities of photoluminescence experiments.

Competing Interests

The authors declare that no competing financial interests or personal relationships influenced the work reported in this paper.

Author Contributions

Patricia F. Silvaino: Photocatalysts preparation and characterization, photochemical experiments, data curation, editing, review. João C. Ferreira: Vinasse treatments, editing, review. Saulo A. Carminati: Data curation, writing-original draft, editing, review, proofreading manuscript; Jorge M. Vaz: Conceptualization, investigation, data curation, supervision, editing, review; Estevam V. Spinacé: Conceptualization,

investigation, data curation, supervision, writing-original draft, editing, review, proofreading. A*ll authors commented on previous versions of the manuscript. All authors read and approved the final manuscript.*

Data Availability

The data that support the findings of this study are available from the authors.

References

1. Rego, G.C., Ferreira, T.B., Ramos, L.R., de Menezes, C.A., Soares, L.A., Sakamoto, I.K., Varesche, M.B.A., Silva, E.L.: Bioconversion of pretreated sugarcane vinasse into hydrogen: new perspectives to solve one of the greatest issues of the sugarcane biorefinery. Biomass Convers Biorefin. 12, 5527–5541 (2022). https://doi.org/10.1007/s13399-020-00984-8
2. Silverio, M.S., Calegari, R.P., Leite, G.M.F.L., Prado, L.M.L.M., Martins, B.C., da Silva, E.A., Neto, J.P., Gomig, A., Baptista, A.S.: Vinasse From the Brazilian Lignocellulosic Ethanol Process: Chemical Composition and Potential for Bioprocesses. Brazilian Journal of Biosystems Engineering. 15, 42–68 (2021). https://doi.org/10.18011/bioeng2021v15n1p42-68
3. Montiel-Rosales, A., Montalvo-Romero, N., García-Santamaría, L.E., Sandoval-Herazo, L.C., Bautista-Santos, H., Fernández-Lambert, G.: Post-Industrial Use of Sugarcane Ethanol Vinasse: A Systematic Review. Sustainability. 14, 11635 (2022). https://doi.org/10.3390/su141811635
4. de Carvalho, J.C., de Souza Vandenberghe, L.P., Sydney, E.B., Karp, S.G., Magalhães, A.I., Martinez-Burgos, W.J., Medeiros, A.B.P., Thomaz-Soccol, V., Vieira, S., Letti, L.A.J., Rodrigues, C., Woiciechowski, A.L., Soccol, C.R.: Biomethane Production from Sugarcane Vinasse in a Circular Economy: Developments and Innovations. Fermentation. 9, 349 (2023). https://doi.org/10.3390/fermentation9040349
5. Nascimento, L.L., Carvalho Souza, R.A., Zacour Marinho, J., Wang, C., Patrocinio, A.O.T.: Light-driven conversion of biomass-derived compounds into green fuels and chemicals. J Clean Prod. 449, 141709 (2024). https://doi.org/10.1016/j.jclepro.2024.141709
6. Montiel-Rosales, A., Montalvo-Romero, N., García-Santamaría, L.E., Sandoval-Herazo, L.C., Bautista-Santos, H., Fernández-Lambert, G.: Post-Industrial Use of Sugarcane Ethanol Vinasse: A Systematic Review. Sustainability. 14, 11635 (2022). https://doi.org/10.3390/su141811635
7. Shi, C., Kang, F., Zhu, Y., Teng, M., Shi, J., Qi, H., Huang, Z., Si, C., Jiang, F., Hu, J.: Photoreforming lignocellulosic biomass for hydrogen production: Optimized design of photocatalyst and photocatalytic system. Chemical Engineering Journal. 452, 138980 (2023). https://doi.org/10.1016/j.cej.2022.138980
8. Zhang, T., Lu, S.: Sacrificial agents for photocatalytic hydrogen production: Effects, cost, and development. Chem Catalysis. 2, 1502–1505 (2022). https://doi.org/10.1016/j.checat.2022.06.023
9. Davis, K.A., Yoo, S., Shuler, E.W., Sherman, B.D., Lee, S., Leem, G.: Photocatalytic hydrogen evolution from biomass conversion. Nano Converg. 8, 6 (2021). https://doi.org/10.1186/s40580-021-00256-9

10. Zhang, G., Ni, C., Huang, X., Welgamage, A., Lawton, L.A., Robertson, P.K.J., Irvine, J.T.S.: Simultaneous cellulose conversion and hydrogen production assisted by cellulose decomposition under UV-light photocatalysis. Chemical Communications. 52, 1673–1676 (2016). https://doi.org/10.1039/C5CC09075J
11. Zhao, H., Liu, J., Zhong, N., Larter, S., Li, Y., Kibria, M.G., Su, B., Chen, Z., Hu, J.: Biomass Photoreforming for Hydrogen and Value-Added Chemicals Co-Production on Hierarchically Porous Photocatalysts. Adv Energy Mater. 13, (2023). https://doi.org/10.1002/aenm.202301828
12. Ma, J., Liu, K., Yang, X., Jin, D., Li, Y., Jiao, G., Zhou, J., Sun, R.: Recent Advances and Challenges in Photoreforming of Biomass-Derived Feedstocks into Hydrogen, Biofuels, or Chemicals by Using Functional Carbon Nitride Photocatalysts. ChemSusChem. 14, 4903–4922 (2021). https://doi.org/10.1002/cssc.202101173
13. Xu, X., Shi, L., Zhang, S., Ao, Z., Zhang, J., Wang, S., Sun, H.: Photocatalytic reforming of lignocellulose: A review. Chemical Engineering Journal. 469, 143972 (2023). https://doi.org/10.1016/j.cej.2023.143972
14. Wongyongnoi, P., Serivalsatit, K., Hunsom, M., Pruksathorn, K.: Simultaneous green synthesis of H_2 and decolorization of distillery effluent by photocatalysis via gold-decorated TiO_2 photocatalysts. Int J Hydrogen Energy. 80, 646–658 (2024). https://doi.org/10.1016/j.ijhydene.2024.07.114
15. Spinacé, E. V., Neto, A.O., Vasconcelos, T.R.R., Linardi, M.: Electro-oxidation of ethanol using PtRu/C electrocatalysts prepared by alcohol-reduction process. J Power Sources. 137, 17–23 (2004). https://doi.org/10.1016/j.jpowsour.2004.05.030
16. Spinacé, E. V., Neto, A.O., Franco, E.G., Linardi, M., Gonzalez, E.R.: Methods of preparation of metal nanoparticles supported on high surface area carbon as electrocatalysts in proton exchange membrane fuel cells. Quim Nova. 27, 648–654 (2004). https://doi.org/10.1590/s0100-40422004000400020
17. Dong, B., Liu, T., Li, C., Zhang, F.: Species, engineering and characterizations of defects in TiO2-based photocatalyst. Chinese Chemical Letters. 29, 671–680 (2018). https://doi.org/10.1016/j.cclet.2017.12.002
18. Shi, J., Chen, J., Feng, Z., Chen, T., Lian, Y., Wang, X., Li, C.: Photoluminescence characteristics of TiO_2 and their relationship to the photoassisted reaction of water/methanol mixture. Journal of Physical Chemistry C. 111, 693–699 (2007). https://doi.org/10.1021/jp065744z
19. Das, R.S., Agrawal, Y.K.: Raman spectroscopy: Recent advancements, techniques and applications. Vib Spectrosc. 57, 163–176 (2011). https://doi.org/10.1016/j.vibspec.2011.08.003
20. Lagopati, N., Tsilibary, E.P., Falaras, P., Papazafiri, P., Pavlatou, E.A., Kotsopoulou, E., Kitsiou, P.: Effect of nanostructured TiO_2 crystal phase on photoinduced apoptosis of breast cancer epithelial cells. Int J Nanomedicine. 9, 3219–3230 (2014). https://doi.org/10.2147/IJN.S62972
21. Lou, Y., Xu, J., Zhang, Y., Pan, C., Dong, Y., Zhu, Y.: Metal-support interaction for heterogeneous catalysis: from nanoparticles to single atoms. Mater Today Nano. 12, (2020). https://doi.org/10.1016/j.mtnano.2020.100093

22. Wang, X., Huang, S.C., Huang, T.X., Su, H.S., Zhong, J.H., Zeng, Z.C., Li, M.H., Ren, B.: Tip-enhanced Raman spectroscopy for surfaces and interfaces. Chem Soc Rev. 46, 4020–4041 (2017). https://doi.org/10.1039/c7cs00206h
23. Haselmann, G.M., Eder, D.: Early-Stage Deactivation of Platinum-Loaded TiO_2 Using In Situ Photodeposition during Photocatalytic Hydrogen Evolution. ACS Catal. 7, 4668–4675 (2017). https://doi.org/10.1021/acscatal.7b00845
24. Wolthuis, Enno., Kolk, Stephen., Schaap, Luke.: Quantitative Estimation of Aromatic Nitro Compounds. Anal Chem. 26, 1238–1240 (1954). https://doi.org/10.1021/ac60091a050
25. Gopakumar, A., Ren, P., Chen, J., Manzolli Rodrigues, B.V., Vincent Ching, H.Y., Jaworski, A., Doorslaer, S. Van, Rokicińska, A., Kuśtrowski, P., Barcaro, G., Monti, S., Slabon, A., Das, S.: Lignin-Supported Heterogeneous Photocatalyst for the Direct Generation of H_2 O $_2$ from Seawater. J Am Chem Soc. 144, 2603–2613 (2022). https://doi.org/10.1021/jacs.1c10786
26. Li, H., Zhu, B., Sun, J., Gong, H., Yu, J., Zhang, L.: Photocatalytic hydrogen production from seawater by TiO2/RuO2 hybrid nanofiber with enhanced light absorption. J Colloid Interface Sci. 654, 1010–1019 (2024). https://doi.org/10.1016/j.jcis.2023.10.074
27. Iervolino, G., Sannino, D., Pepe, G., Giovanna Basilicata, M., Campiglia, P., Vaiano, V.: An effective way for the simultaneous valorization and treatment of olive mill wastewater by means of a photocatalytic process. Chemical Engineering Journal. 468, 143725 (2023). https://doi.org/10.1016/j.cej.2023.143725
28. Skliri, E., Vamvasakis, I., Papadas, I.T., Choulis, S.A., Armatas, G.S.: Mesoporous composite networks of linked $MnFe_2O_4$ and $ZnFe_2O_4$ nanoparticles as efficient photocatalysts for the reduction of cr(vi). Catalysts. 11, 1–16 (2021). https://doi.org/10.3390/catal11020199

Figures

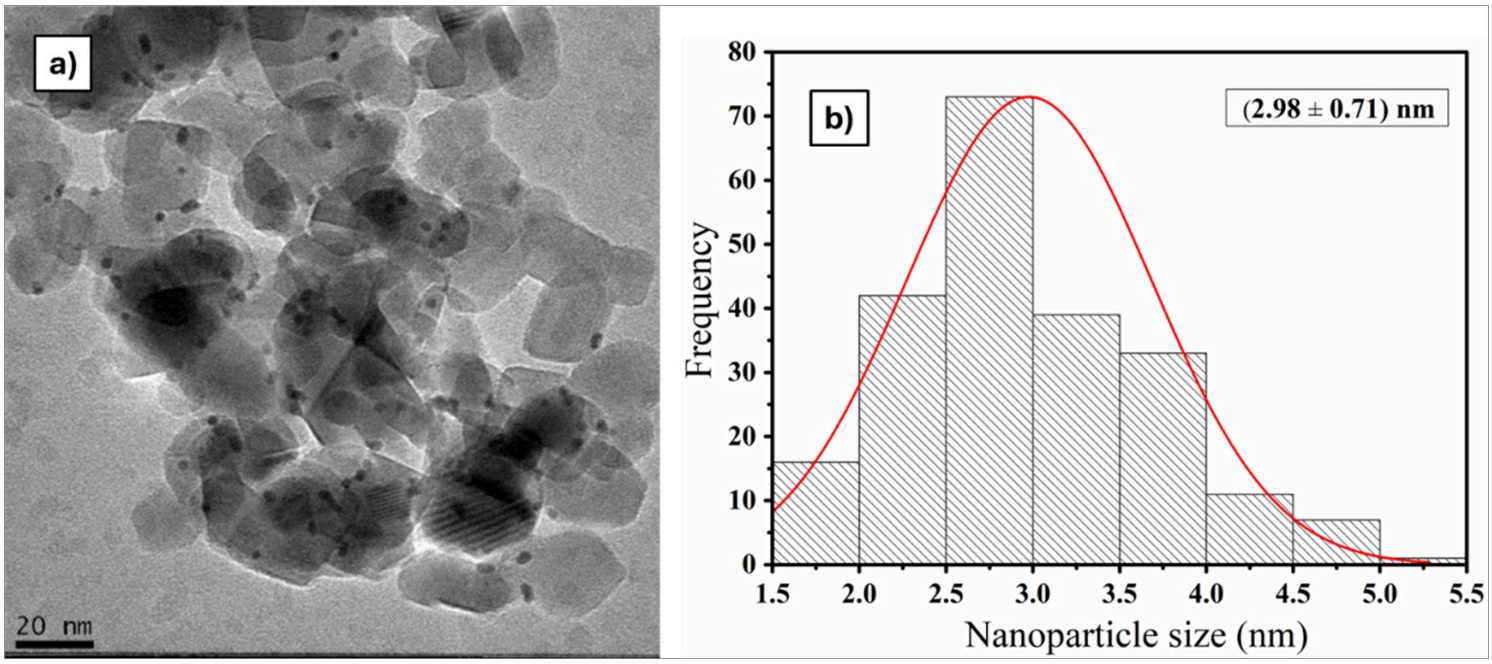

Figure 1

a) TEM micrograph and b) histogram of Pt/TiO2 photocatalyst

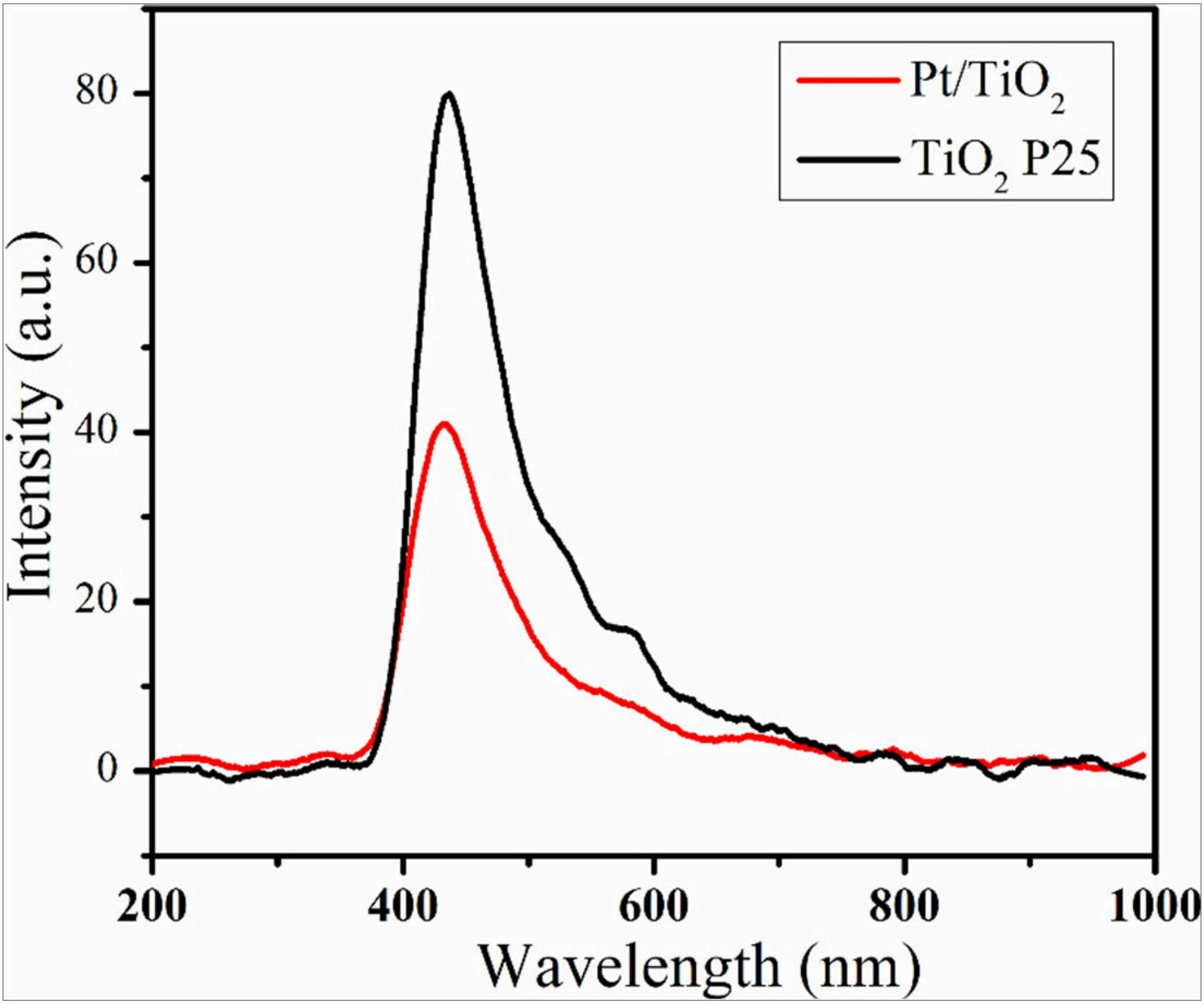

Figure 2

PL spectra of TiO_2 P25 commercial and Pt/TiO_2 photocatalyst

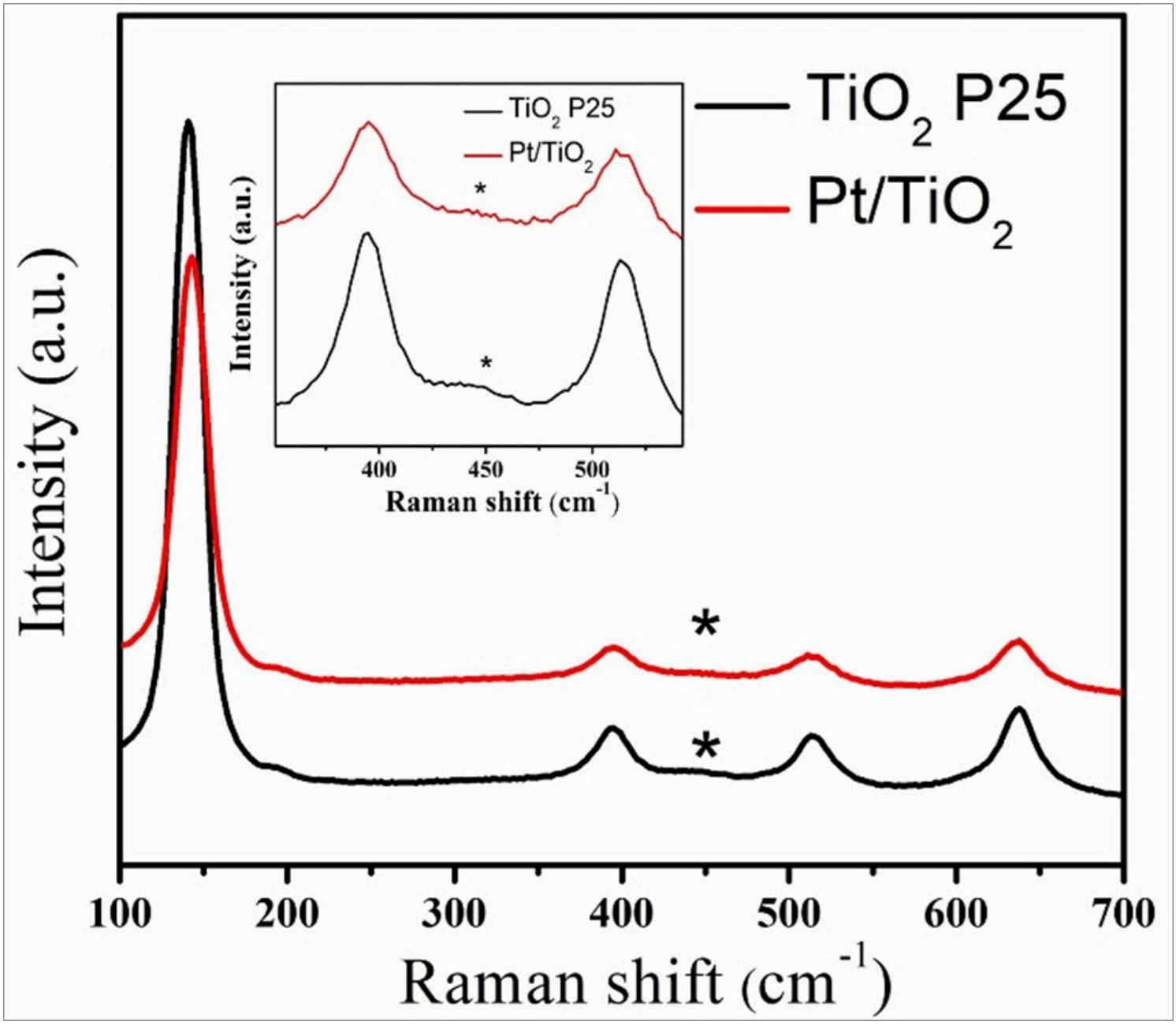

Figure 3

Raman spectra of commercial TiO_2 P25 and Pt/TiO_2 photocatalyst

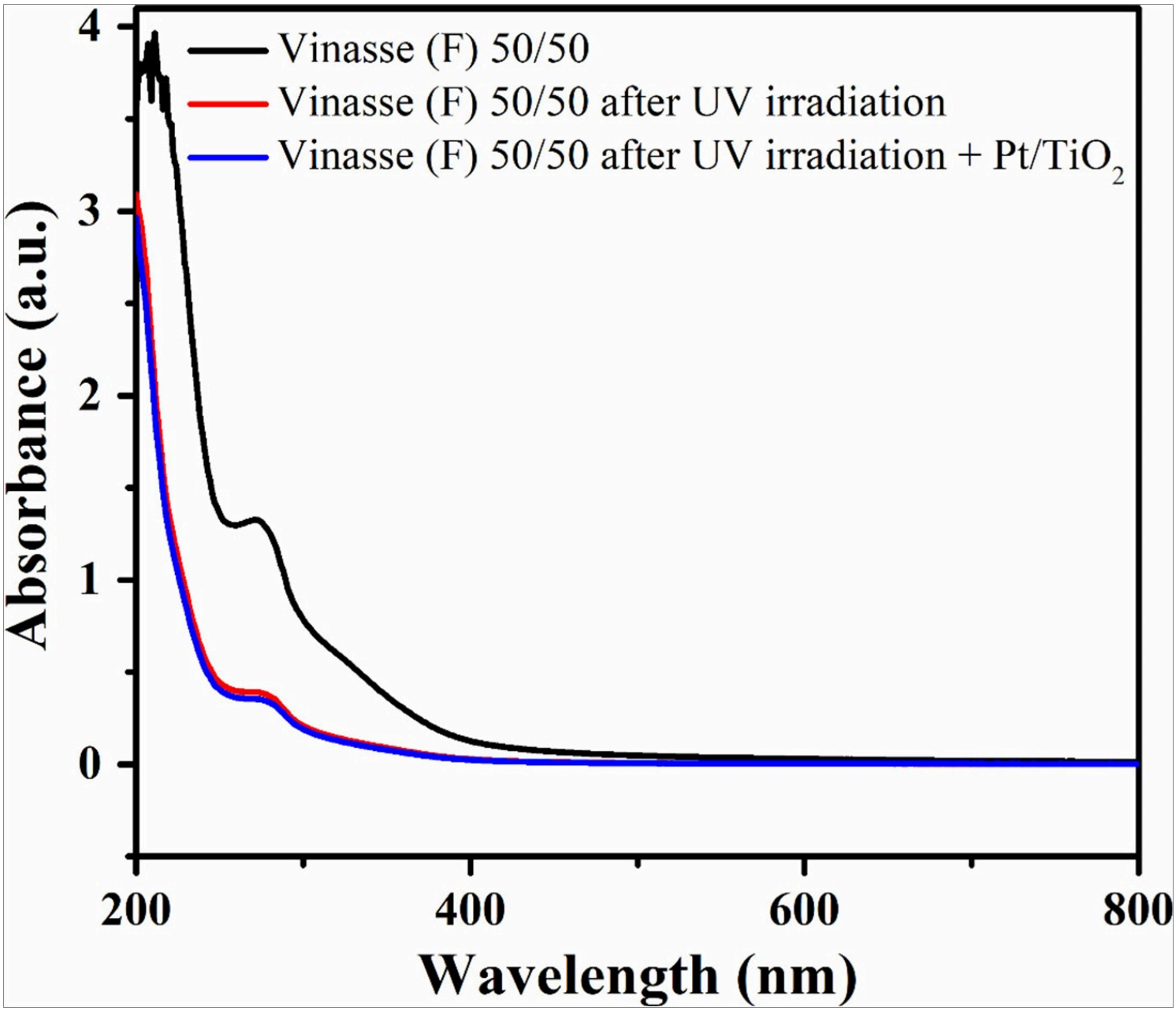

Figure 4

UV-Vis absorption spectra of Vinasse (F) SA/H_2O of 50/50, after UV irradiation and after UV irradiation in the presence of Pt/TiO_2

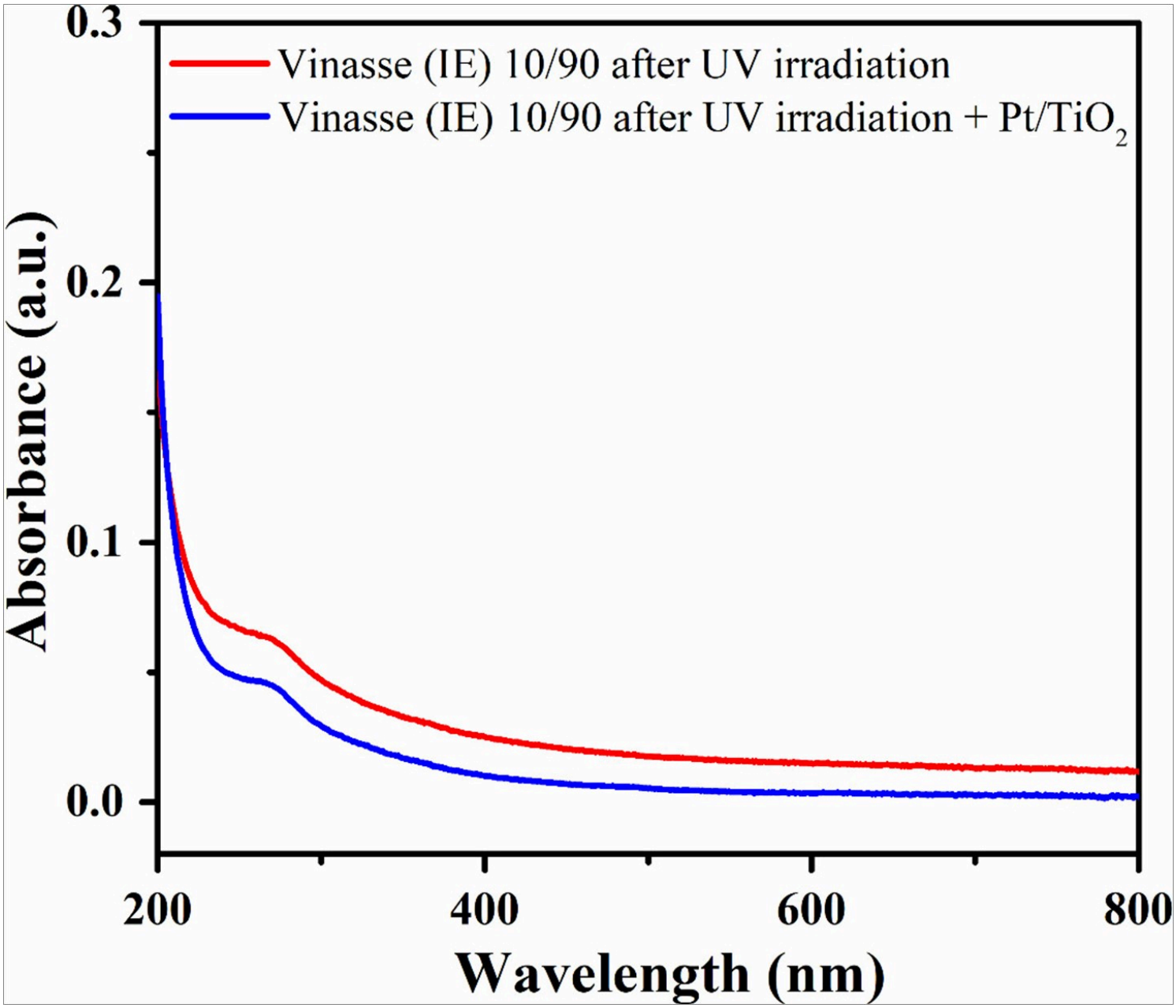

Figure 5

UV-Vis absorption spectra of Vinasse (IE) SA/H_2O of 10/90 after UV irradiation and after UV irradiation in the presence of Pt/TiO_2